

First-principles calculations of steering forces in epitaxial growth

Jianguo Yu and Jacques G. Amar

Department of Physics & Astronomy, University of Toledo, Toledo, Ohio 43606, USA

Alexander Bogicevic

Scientific Research Laboratories, Ford Motor Company, Dearborn, Michigan 48124, USA

(Received 24 July 2003; revised manuscript received 23 December 2003; published 23 March 2004)

Although atoms deposited during epitaxial growth strongly prefer to bind to step bottoms of existing islands, the geometrical proximity of step tops can lead to atoms landing there instead, significantly altering film morphology and contributing to growth instabilities. To shed light on such steering effects, we have mapped out the three-dimensional static potential-energy surface (PES) for Cu atoms approaching a stepped Cu(100) surface using density-functional theory (DFT). Depending on the kinetic energy of incident atoms, surface relaxations may be too sluggish, and we have therefore computed the PES both with and without allowing substrate relaxations. While a comparison with the corresponding embedded-atom-method (EAM) results indicates relatively good agreement, the DFT calculations suggest that the steering effect is slightly weaker than predicted by EAM calculations. These results also support a previous comparison with experiment, which indicated that the overall funneling probability for deposition at a [110] step edge on the Cu(100) surface is close to but slightly lower than that predicted via EAM simulations.

DOI: 10.1103/PhysRevB.69.113406

PACS number(s): 81.15.Aa, 68.55.-a, 81.10.Aj

I. INTRODUCTION

One particularly important process controlling the evolution of the surface morphology in epitaxial growth is the accommodation of incoming atoms deposited near steps. For example, in metal epitaxial growth, the energy of condensation of depositing atoms is believed to lead to “downward funneling,”¹ i.e., atoms deposited beyond the edge of a step “funnel” to the bottom terrace while atoms deposited on the “uphill” side go to the upper terrace. Such processes lead to a downhill current which tends to stabilize the surface. In the case of unstable growth [due either to an Ehrlich-Schwoebel (ES) barrier² to the descent of diffusing atoms at steps, or to step-atom attraction^{3,4} or to step-edge diffusion⁵] the resulting balance between uphill and downhill currents leads to slope selection.⁶ Analytical calculations⁴ indicate that the surface current and selected mound slope depend strongly on the “bias” for atoms landing near a step.

Recently, we have carried out molecular-dynamics (MD) simulations using Voter-Chen embedded-atom-method (EAM) potentials⁷ for Cu/Cu(100) and Ag/Ag(100) deposition near a step edge in order to study the effects of short-range attraction in epitaxial growth.⁸ In our Cu/Cu(100) simulations,⁸ Cu atoms were deposited over a range of distances x (where $0 < x < a_1$ and $a_1 = 2.55 \text{ \AA}$ is the nearest-neighbor distance) beyond the edge of a [110] step on the Cu(100) substrate, and their trajectories followed in order to determine whether or not they landed on the upper and lower terrace. For both Cu/Cu(100) and Ag/Ag(100), our simulation results⁸ led to a picture of the process of deposition near step edges which is quite different from the standard downward funneling picture. In particular, they indicated that in metal epitaxial growth the short-range attraction of depositing atoms to step edges can indeed lead to significant uphill funneling—i.e., atoms deposited beyond the step edge may land on the upper terrace rather than the lower terrace. As we

have shown,⁸ in the presence of an ES barrier, this leads to a significant increase in the selected mound angle and surface roughness in the case of unstable epitaxial growth. In particular, we have used our Cu/Cu(100) deposition results to accurately predict the experimental mound angle (corresponding to {113} facets) and surface roughness observed in recent experiments.⁹

The relatively good agreement⁸ between our uphill funneling results for Cu/Cu(100) obtained using an EAM potential, and those obtained using an effective Lennard-Jones Cu potential suggests that in this case the degree of uphill funneling is only weakly dependent on the details of the potential. However, it is clearly desirable to check if these results agree with the predictions of first-principles calculations. This is the primary goal of this paper, and accordingly, here we present a comparison between density-functional theory (DFT) calculations and EAM calculations for the interaction between a depositing atom and a step edge.

We note that in our previous work we found that for typical energies in epitaxial growth, significant effects of the short-range attraction occur both after as well as before the atom has collided with the step and lost its kinetic energy of condensation. Unfortunately, it is extremely prohibitive computationally to carry out the *ab initio* MD simulations required to study the interaction after the atom has collided with the step. Therefore, here we focus on a comparison between the predictions of the DFT and EAM potentials for the attractive (steering) portion of the interaction. In particular, we present a comparison between density-functional theory and EAM calculations for the force and potential-energy surface (PES) for an atom near a step edge for the case of Cu/Cu(100).

II. DETAILS OF CALCULATION

In order to test our EAM results for the short-range attraction near a step edge, we have carried out first-principles

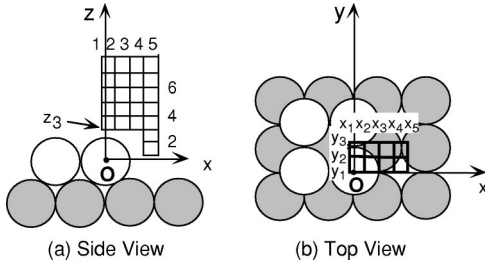


FIG. 1. Diagram showing side (a) and top (b) views of portion of top two layers of supercell along with $3 \times 5 \times 6$ grid of points used in DFT calculations.

calculations for the static potential energy and forces acting on a Cu atom as it approaches the step. These calculations are based on DFT as implemented in the VASP code.¹⁰ For the exchange-correlation functional, the Perdew-Wang PW91 implementation of the generalized gradient approximation (Ref. 11) is employed. The one-electron wave functions are expanded in a plane-wave basis with an energy cutoff of 29.1 Ry. Ultrasoft Vanderbilt pseudopotentials¹² are used to describe the electron core-valence interactions. The Kohn-Sham equations are solved self-consistently, and the atomic structure is optimized until residual forces on all unconstrained atoms are less than $0.03 \text{ eV}/\text{\AA}$. To improve convergence, the Methfessel-Paxton Fermi-level smearing¹³ is used with a Gaussian width of 0.2 eV. The Brillouin zone is sampled with a uniform 4×2 k -point Monkhorst-Pack mesh. Except for specific tests discussed below, all calculations carried out were non-spin-polarized. The supercell used in the DFT calculations corresponds to $5 \frac{1}{2}$ layers of fcc Cu(100) at zero temperature. Each full layer consisted of a 3-atom by 6-atom slab, while the top half layer (corresponding to the step) consisted of a 3-atom by 3-atom slab. Periodic boundary conditions were assumed in the horizontal directions. The starting point of all calculations is a fully relaxed slab corresponding to a stepped Cu(100) surface, with the bottom two layers always kept fixed at bulk crystal positions. An additional atom was positioned in the vacuum above this slab at various locations (as described in detail below), and the potential energy landscape and forces acting on this fixed atom were mapped out.

Due to interactions between the impinging atom and the substrate, there is always some local substrate relaxation that alters the potential energy and forces. Because of the dynamical nature of the deposition, it is not *a priori* clear whether there is sufficient time for full substrate relaxation to occur during the deposition process. Accordingly, we have carried out two sets of static DFT calculations to bracket the extremes of an infinitely sluggish substrate (“unrelaxed” system) and an instantly responsive substrate (“relaxed” system). In the former case, no further relaxation of the slab is allowed, and the energy and forces at various points in the vacuum above the stepped surface are recorded. In the second case, a complete relaxation of the top $3 \frac{1}{2}$ layers of the stepped surface was allowed for every individual position of the depositing atom. Far away from the surface, both the energies and forces for the two cases are the same.

In order to compare with DFT results, EAM calculations

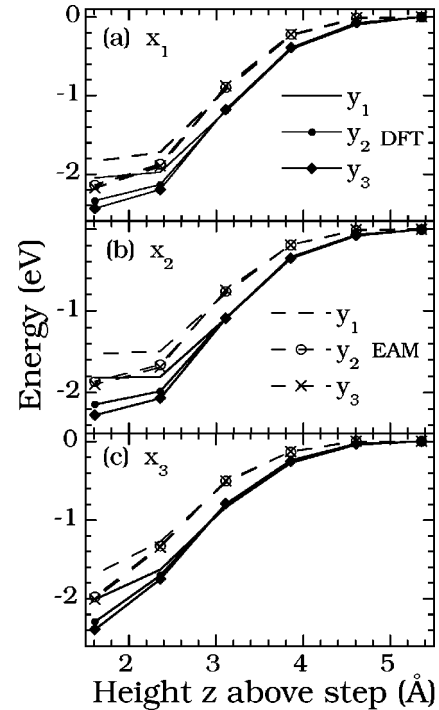


FIG. 2. Potential-energy curves $U(z)$ for (a) x_1 , (b) x_2 , and (c) x_3 for three different values of y along the step edge for the case of a relaxed substrate. Solid lines, filled symbols correspond to DFT results while dashed lines, open symbols correspond to EAM results.

were also carried out using the same atomic configurations (in the unrelaxed case) and grid positions as in the DFT calculations. In our relaxed EAM calculations, the top $3 \frac{1}{2}$ layers of the initial DFT configuration were allowed to relax in the presence of the “depositing” atom, while the bottom two layers were held fixed. In all cases, the reference energy or zero of energy was taken to correspond to large z , i.e., the depositing atom infinitely far away from the substrate.

As shown in Fig. 1, the potential energy and forces on an incoming atom were calculated at a set of 102 positions (x, y, z) corresponding to a $5 \times 3 \times 6$ cubic grid of points above the step edge, plus a $2 \times 3 \times 2$ cubic grid of points next to the step ($x = 1 - 3$ are not considered for $z = 1 - 2$ because of interference with step atoms). Here, x , y , and z correspond to positions across, along, and above the step edge, respectively, while the grid spacing was given by $\Delta = 0.75 \text{ \AA}$. Taking the origin O of our coordinate system as shown in Fig. 1, one has $x_1 = -0.07a_1 \approx -0.18 \text{ \AA}$, $y_1 = 0$, $z_1 = 0.108 \text{ \AA}$. We note that while x_1 corresponds to a position slightly on the uphill side of the upper terrace, x_2 corresponds to an initial distance from the step edge ($0.22a_1$) at which significant uphill funneling was observed in our EAM molecular-dynamics simulations.^{8,14} At position $x_3 = 0.51a_1$ the atom is too far away from the step and always lands on the lower terrace. Similarly, position y_1 corresponds to a “top” position while y_2 and y_3 correspond to slight deviations from the “mid” position between two atoms on the step edge. The lowest z point in our grid above the step corresponds to $z_3 = 1.6 \text{ \AA} = 0.63a_1$ above the step.

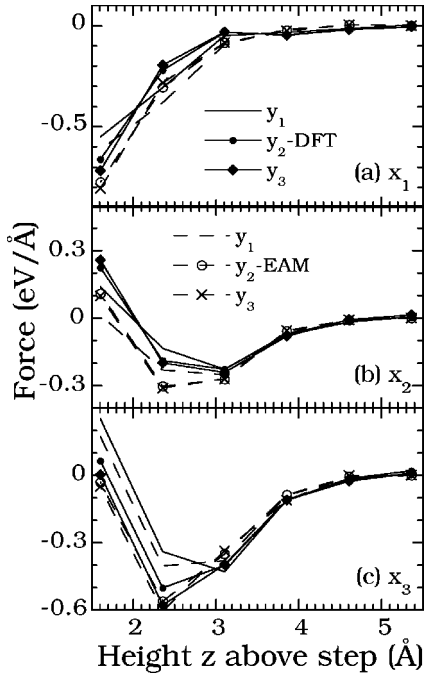


FIG. 3. Steering force F_x as a function of height z above the step edge for (a) x_1 , (b) x_2 , and (c) x_3 for three different values of y along the step edge for the case of a relaxed substrate. Solid lines, filled symbols correspond to DFT results while dashed lines, open symbols correspond to EAM results.

III. RESULTS

A. Relaxed substrate

Figure 2 shows a comparison between our DFT results (closed symbols, solid lines) and the corresponding EAM results (open symbols, dashed lines) for the total system potential energy as a function of height z above the top layer for the three distances x_1, x_2 , and x_3 closest to the step edge and three different positions y along the step edge for each value of x . As can be seen, while the two potential curves are quite similar for all nine different values of x and y , the depth of the EAM potential well is typically approximately 10% lower than the DFT potential well. This implies that for a fully relaxed substrate the EAM potential somewhat underestimates the gain in kinetic energy as atoms approach a step edge. This in turn suggests that for the fully relaxed substrate the steering effect due to short-range attraction is likely to be somewhat weaker than predicted by our EAM calculations.

The corresponding results for the component F_x of the steering force perpendicular to the step are shown in Fig. 3. In all cases, the EAM prediction for the steering force is *slightly* stronger for small z (i.e., close to the step) than the DFT calculation. Combined with the results of Fig. 2, this implies that, although there is relatively good agreement between the DFT and EAM energies, the EAM potential most likely somewhat overestimates the strength of the steering effect for the case of a relaxed substrate.

B. Unrelaxed substrate

We now consider the corresponding results for an unrelaxed substrate. As shown in Fig. 4, due to the lack of relax-

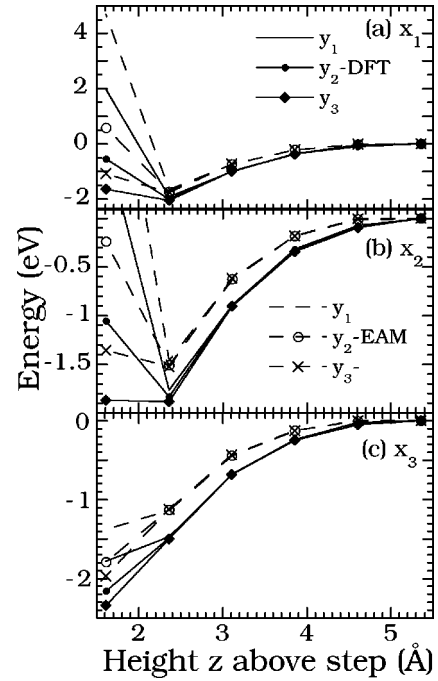


FIG. 4. Same as Fig. 2 but for unrelaxed substrate.

ation the depth of the potential well is slightly lower than for the relaxed case. As for the relaxed substrate, the EAM potential well is somewhat shallower than the DFT potential well. (For x_1 near the step edge they are comparable, however for x_2 and x_3 beyond the step edge there is a clear difference.) As for the relaxed substrate, this implies that the steering effect due to short-range attraction is likely to be somewhat weaker than predicted by our EAM calculations.

As shown in Fig. 5, the DFT and EAM predictions for the

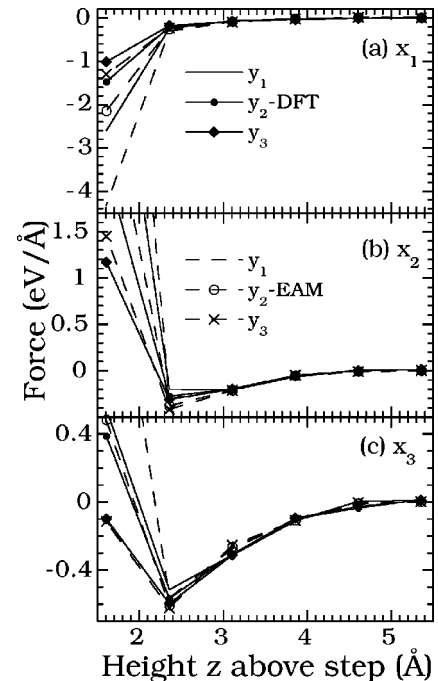


FIG. 5. Same as Fig. 3 but for unrelaxed substrate.

steering force are also very similar, except for very small z . In particular, for x_2 and x_3 (beyond the step edge) and small z , the DFT prediction for the attractive steering force perpendicular to the step is almost identical to the EAM prediction,¹⁵ while for very small z the repulsive steering force is somewhat *weaker* than predicted by the EAM potential. This indicates that the overall difference between the DFT and EAM predictions for the steering effect in the case of an unrelaxed substrate is even smaller than for the relaxed case.

IV. CONCLUSION

We have carried out a quantitative comparison between *ab initio* calculations for the static potential-energy surface and steering forces for an atom approaching a Cu[110] step edge, and the corresponding EAM calculations, in order to assess the validity of our EAM-based molecular-dynamics simulations of deposition at steps. Our results indicate that for both the unrelaxed and relaxed substrate cases, there is relatively little difference between the EAM and DFT predictions for the steering force F_x and the potential-energy surface. However, the DFT prediction for the binding energy is somewhat higher than the EAM prediction, while the at-

tractive steering force F_x is generally somewhat weaker. These results support the conclusions of our previous EAM MD simulations⁸ in which we found that uphill funneling due to short-range attraction may play a significant role in metal (100) epitaxial growth. These results also support our conclusions that an uphill funneling probability close to that obtained in our EAM MD simulations may be used to explain recent experiments on Cu/Cu(100) growth.⁹ We note that in this case the value of the uphill funneling probability ($P_{up} \approx 0.55$) obtained from our EAM MD simulations, led to a value of the surface roughness obtained from kinetic Monte Carlo simulations which was actually slightly higher than the experimental value. This is in agreement with our observation that the DFT results are close to but somewhat weaker than the EAM results.

ACKNOWLEDGMENTS

This work was supported by a grant from the Petroleum Research Fund of the American Chemical Society. We would like to thank Art Voter for providing us with the EAM embedding functions for Cu as well as the Ohio Supercomputer Center for a grant of computer time.

¹J.W. Evans, D.E. Sanders, P.A. Thiel, and A.E. DePristo, Phys. Rev. B **41**, 5410 (1990); H.C. Kang and J.W. Evans, Surf. Sci. **271**, 321 (1992).

²G. Ehrlich and F. Hudda, J. Chem. Phys. **44**, 1039 (1966); R.L. Schwoebel, J. Appl. Phys. **40**, 614 (1969).

³S.C. Wang and G. Ehrlich, Phys. Rev. Lett. **70**, 41 (1993).

⁴J.G. Amar and F. Family, Phys. Rev. B **54**, 14 071 (1996); Phys. Rev. Lett. **77**, 4584 (1996).

⁵M.V. Ramana Murty and B.H. Cooper, Phys. Rev. Lett. **83**, 352 (1999).

⁶M. Siegert and M. Plischke, Phys. Rev. Lett. **73**, 1517 (1994); Phys. Rev. E **53**, 307 (1996).

⁷A.F. Voter, Proc. SPIE **821**, 214 (1987); Los Alamos Unclassified Technical Report No. LA-UR-93-3901.

⁸J. Yu and J.G. Amar, Phys. Rev. Lett. **89**, 286103 (2002).

⁹H.-J. Ernst, F. Fabre, R. Folkerts, and J. Lapujoulade, Phys. Rev.

Lett. **72**, 112 (1994).

¹⁰G. Kresse and J. Hafner, Phys. Rev. B **47**, 558 (1993); **49**, 14 251 (1994); G. Kresse and J. Furthmüller, Comput. Mater. Sci. **6**, 15 (1996); Phys. Rev. B **54**, 11 169 (1996).

¹¹J. P. Perdew, in *Electronic Structure of Solids '91*, edited by P. Ziesche and H. Eschrig (Akademie Verlag, Berlin, 1991); J. P. Perdew and Y. Wang (unpublished).

¹²D. Vanderbilt, Phys. Rev. B **41**, 7892 (1990).

¹³M. Methfessel and A.T. Paxton, Phys. Rev. B **40**, 3616 (1989).

¹⁴For $K_i \approx 0.23$ eV corresponding to the typical incident kinetic energy for epitaxial Cu deposition, the critical distance was $x_c/a_1 \approx 0.3$.

¹⁵For $x = x_1$ very near the step edge, the DFT force is again weaker than the EAM prediction. However, in this case there is no difference in the degree of uphill funneling since the atom is already on the "top" side of the step edge.